Chapter 4

Three-dimensional Delaunay triangulations

Three-dimensional triangulations are sometimes called tetrahedralizations. Delaunay tetrahedralizations are not quite as effective as planar Delaunay triangulations at producing elements of good quality, but they are nearly as popular in the mesh generation literature as their two-dimensional cousins. Many properties of Delaunay triangulations in the plane generalize to higher dimensions, but many of the optimality properties do not. Notably, Delaunay tetrahedralizations do not maximize the minimum angle (whether plane angle or dihedral angle). Figure 4.1 depicts a three-dimensional counterexample. The hexahedron at the top is the convex hull of its five vertices. The Delaunay triangulation of those vertices, to the left, includes a thin tetrahedron known as a *sliver* or *kite*, whose vertices are nearly coplanar and whose dihedral angles can be arbitrarily close to 0° and 180°. A triangulation of the same vertices that is not Delaunay, at lower right, has better quality.

This chapter surveys Delaunay triangulations and constrained Delaunay triangulations in three—and occasionally higher—dimensions. Constrained Delaunay triangulations generalize uneasily to three dimensions, because there are polyhedra that do not have any tetrahedralization at all.

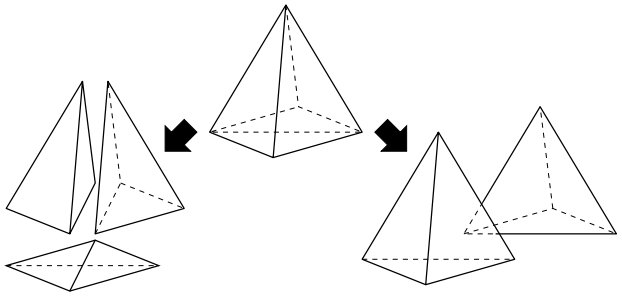

Figure 4.1: This hexahedron has two tetrahedralizations. The Delaunay tetrahedralization at left includes an arbitrarily thin sliver tetrahedron. The non-Delaunay tetrahedralization at right consists of two nicely shaped tetrahedra.

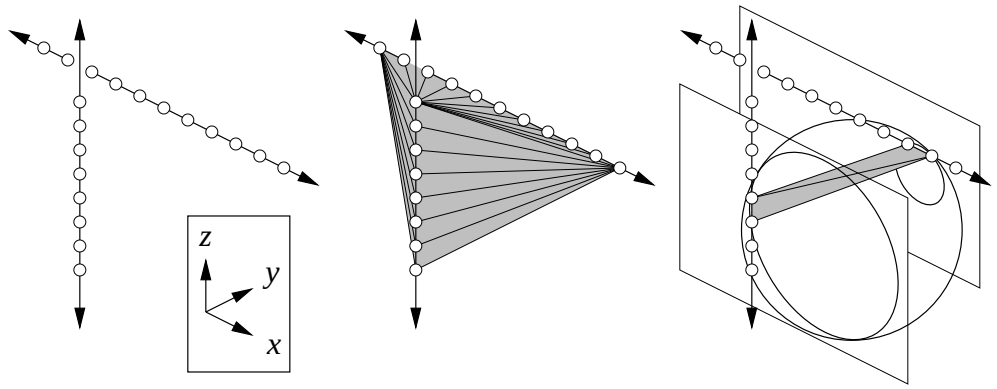

Figure 4.2: At center, the Delaunay tetrahedralization of the points at left. At right, the circumball of one Delaunay tetrahedron with two cross-sections showing it is empty.

4.1 Triangulations of a point set in $\mathbb{R}^d$

Definition 2.1 in Section 2.1 defines a triangulation of a set of points to be a simplicial complex whose vertices are the points and whose union is the convex hull of the points. With no change, the definition holds in any finite dimension d. Figures 4.1–4.4 illustrate triangulations of point sets in three dimensions. Every finite point set in $\mathbb{R}^d$ has a triangulation; for example, the lexicographic triangulation of Section 2.1 also generalizes to higher dimensions with no change.

Let S be a set of n points in $\mathbb{R}^d$. Recall from Section 2.1 that if all the points in S are collinear, they have one triangulation having n vertices and $n-1$ collinear edges connecting them. This is true regardless of d; the triangulation is one-dimensional, although it is embedded in $\mathbb{R}^d$. More generally, if the affine hull of S is k-dimensional, then every triangulation of S is a k-dimensional triangulation embedded in $\mathbb{R}^d$: the simplicial complex has at least one k-simplex but no $(k+1)$-simplex.

The *complexity* of a triangulation is its total number of simplices of all dimensions. Whereas a planar triangulation of n points has $O(n)$ triangles and edges, a surprising property of higher-dimensional triangulations is that they can have superlinear complexity. Figure 4.2 shows a triangulation of n points that has $\Theta(n^2)$ edges and tetrahedra. Every vertex lies on one of two non-intersecting lines, and there is one tetrahedron for each pairing of an edge on one line and an edge on the other. This is the *only* triangulation of these points, and it is Delaunay. In general, a triangulation of n vertices in $\mathbb{R}^3$ has at most $(n^2-3n-2)/2$ tetrahedra, at most n^2-3n triangles, and at most $(n^2-n)/2$ edges. An n-vertex triangulation in $\mathbb{R}^d$ can have a maximum of $\Theta(n^{\lceil d/2 \rceil})$ d-simplices.

4.2 The Delaunay triangulation in $\mathbb{R}^d$

Delaunay triangulations generalize easily to higher dimensions. Let S be a finite set of points in $\mathbb{R}^d$, for $d \geq 1$. Let σ be a k-simplex (for any $k \leq d$) whose vertices are in S. The simplex σ is *Delaunay* if there exists an open circumball of σ that contains no point in S. Clearly, every face of a Delaunay simplex is Delaunay too. The simplex σ is *strongly Delaunay* if there exists

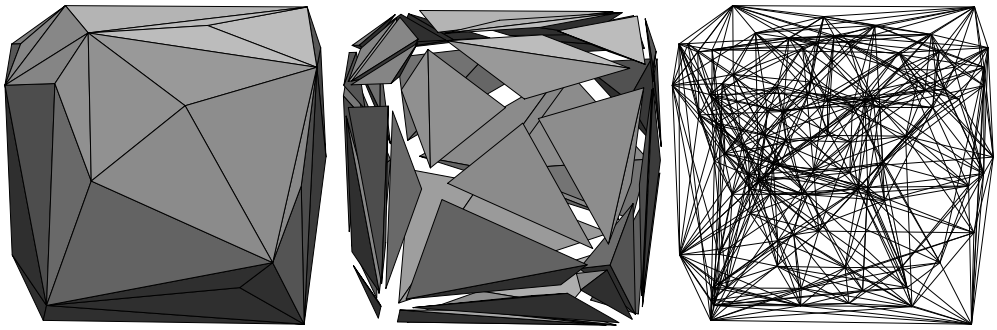

Figure 4.3: Three renderings of a Delaunay tetrahedralization.

a closed circumball of σ that contains no point in S except the vertices of σ. Every point in S is trivially a strongly Delaunay vertex.

Definition 4.1 (Delaunay triangulation)**.** Let S be a finite point set in $\mathbb{R}^d$, and let k be the dimension of its affine hull. A *Delaunay triangulation* $\operatorname{Del} S$ of S is a triangulation of S in which every k-simplex is Delaunay—and therefore, every simplex is Delaunay.

Figure 4.2 depicts a Delaunay tetrahedralization and the empty circumball of one of its tetrahedra. Figure 4.3 depicts a more typical Delaunay tetrahedralization, with complexity linear in the number of vertices.

The parabolic lifting map generalizes to higher dimensions too. It maps each point $p = (p_1, p_2, \ldots, p_d) \in \mathbb{R}^d$ to its *lifted companion*, the point $p^+ = (p_1, p_2, \ldots, p_d, p_1^2 + p_2^2 + \cdots + p_d^2)$ in $\mathbb{R}^{d+1}$. Consider the $(d+1)$-dimensional convex hull of the lifted points, $S^+ = \{v^+ : v \in S\}$. Projecting the downward-facing faces of $\operatorname{conv} S^+$ to $\mathbb{R}^d$ yields a polyhedral complex called the *Delaunay subdivision* of S. If S is *generic*, its Delaunay subdivision is simplicial and S has exactly one Delaunay triangulation.

Definition 4.2 (generic)**.** Let S be a point set in $\mathbb{R}^d$. Let k be the dimension of the affine hull of S. The set S is *generic* if no $k+2$ points in S lie on the boundary of a single d-ball.

If S if not generic, its Delaunay subdivision may have non-simplicial faces; recall Figure 2.3. In that case, S has multiple Delaunay triangulations, which differ according to how the non-simplicial faces are triangulated.

Whereas each non-simplicial face in a two-dimensional Delaunay subdivision can be triangulated independently, in higher dimensions the triangulations are not always independent. Figure 4.4 illustrates a set of twelve points in $\mathbb{R}^3$ whose Delaunay subdivision includes two cubic cells that share a square 2-face. The square face can be divided into two triangles in two different ways, and each cube can be divided into five or six tetrahedra in several ways, but they are not independent: the triangulation of the square face constrains how both cubes are triangulated.

A *least-vertex triangulation* provides one way to safely subdivide a polyhedral complex into a simplicial complex. To construct it, triangulate the 2-faces through the d-faces in order of increasing dimension. To triangulate a non-simplicial k-face f, subdivide it into k-simplices of the form $\operatorname{conv}(v \cup g)$, where v is the lexicographically minimum vertex of f, and g varies over the $(k-1)$-simplices on f's subdivided boundary that do not contain v. The choice of the lexicographically

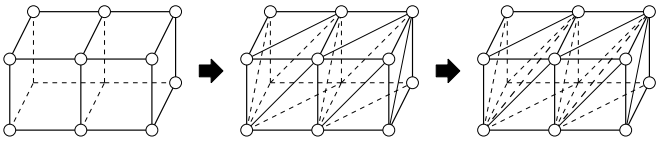

Figure 4.4: A Delaunay subdivision comprising two cubic cells and their faces. The least-vertex Delaunay triangulation subdivides each 2-face into triangles adjoining the face's lexicographically minimum vertex, and likewise subdivides each 3-face into tetrahedra.

minimum vertex of each face ensures that the face triangulations are compatible with each other. The least-vertex triangulation is consistent with the weight perturbations described in Section 2.9.

Many properties of planar Delaunay triangulations discussed in Chapter 2 generalize to higher dimensions. A few of them are summarized below. Proofs are omitted, but each of them is a straightforward extension of the corresponding proof for two dimensions.

Recall that a *facet* of a polyhedral complex is a $(d-1)$-face, and a facet of a triangulation is a $(d-1)$-simplex. The forthcoming Delaunay Lemma provides an alternative definition of a Delaunay triangulation: a triangulation of a point set in which every facet is locally Delaunay. A facet f in a triangulation $\mathcal{T}$ is said to be *locally Delaunay* if it is a face of fewer than two d-simplices in $\mathcal{T}$, or it is a face of exactly two d-simplices τ_1 and τ_2 and it has an open circumball that contains no vertex of τ_1 nor τ_2. Equivalently, the open circumball of τ_1 contains no vertex of τ_2. Equivalently, the open circumball of τ_2 contains no vertex of τ_1.

Lemma 4.1 (Delaunay Lemma)**.** *Let $\mathcal{T}$ be a triangulation of a finite, d-dimensional set S of points in $\mathbb{R}^d$. The following three statements are equivalent.*

- *Every d-simplex in $\mathcal{T}$ is Delaunay (i.e. $\mathcal{T}$ is Delaunay).*
- *Every facet in $\mathcal{T}$ is Delaunay.*
- *Every facet in $\mathcal{T}$ is locally Delaunay.* □

As in the plane, a generic point set has exactly one Delaunay triangulation, composed of every strongly Delaunay simplex. The following three propositions have essentially the same proofs as in Section 2.7.

Proposition 4.2. *Let σ be a strongly Delaunay simplex, and let τ be a Delaunay simplex. Then $\sigma \cap \tau$ is either empty or a shared face of both σ and τ.*

Proposition 4.3. *Every Delaunay triangulation of a point set contains every strongly Delaunay simplex.*

Theorem 4.4. *A generic point set has exactly one Delaunay triangulation.*

4.3 The optimality of the Delaunay triangulation in $\mathbb{R}^d$

Some optimality properties of Delaunay triangulations hold in any dimension. Consider the use of triangulations for piecewise linear interpolation of a quadratic multivariate function. If the

function is isotropic—of the form $\alpha\|p\|^2 + \langle a, p\rangle + \beta$ for $p \in \mathbb{R}^d$—then the Delaunay triangulation minimizes the interpolation error measured in the L_q-norm for every $q \geq 1$, compared with all other triangulations of the same points. (If the function is not isotropic, but it is parabolic rather than hyperbolic, then the optimal triangulation is a weighted Delaunay triangulation in which the function determines the vertex heights.)

Delaunay triangulations also minimize the radius of the largest min-containment ball of their simplices (recall Definition 1.20). This result implies a third optimality result, also related to multivariate piecewise linear interpolation. Suppose one must choose a triangulation to interpolate an unknown function, and one wishes to minimize the largest pointwise error in the domain. After one chooses the triangulation, an adversary will choose the worst possible smooth function for the triangulation to interpolate, subject to a fixed upper bound on the absolute curvature (i.e. second directional derivative) of the function anywhere in the domain. The Delaunay triangulation is the optimal choice.

To better understand these three optimality properties, consider multivariate piecewise linear interpolation on a triangulation $\mathcal{T}$ of a point set S. Let $\mathcal{T}^+ = \{\sigma^+ : \sigma \in \mathcal{T}\}$ be the triangulation lifted by the parabolic lifting map; $\mathcal{T}^+$ is a simplicial complex embedded in $\mathbb{R}^{d+1}$. Think of $\mathcal{T}^+$ as inducing a continuous piecewise linear function $\mathcal{T}^+(p)$ that maps each point $p \in \operatorname{conv} S$ to a real value.

How well does $\mathcal{T}^+$ approximate the paraboloid? Let $e(p) = \mathcal{T}^+(p) - \|p\|^2$ be the error in the interpolated function $\mathcal{T}^+$ as an approximation of the paraboloid $\|p\|^2$. At each vertex $v \in S$, $e(v) = 0$. Because $\|p\|^2$ is convex, the error satisfies $e(p) \geq 0$ for all $p \in \operatorname{conv} S$.

Proposition 4.5. *At every point $p \in \operatorname{conv} S$, every Delaunay triangulation $\mathcal{T}$ of S minimizes $\mathcal{T}^+(p)$, and therefore minimizes the interpolation error $e(p)$, among all triangulations of S. Hence, every Delaunay triangulation of S minimizes $\|e\|_{L_q}$ for every Lebesgue norm L_q, and every other norm monotonic in e.*

P . If $\mathcal{T}$ is Delaunay, then $\mathcal{T}^+$ is the set of faces of the underside of the convex hull $\operatorname{conv} S^+$ of the lifted vertices (or a subdivision of those faces if some of them are not simplicial). No simplicial complex in $\mathbb{R}^{d+1}$ whose vertices are all in S^+ can pass through any point below $\operatorname{conv} S^+$. □

Proposition 4.6. *Let o and r be the circumcenter and circumradius of a d-simplex σ. Let o_{mc} and r_{mc} be the center and radius of the min-containment ball of σ. Let q be the point in σ nearest o. Then $o_{\mathrm{mc}} = q$ and $r_{\mathrm{mc}}^2 = r^2 - d(o, q)^2$.*

P . Let τ be the face of σ whose relative interior contains q. The face τ is not a vertex, because the vertices of σ are σ's furthest points from o. Because q is the point in τ nearest o, and because q is in the relative interior of τ, the line segment oq is orthogonal to τ. (This is true even if $\tau = \sigma$, in which case $o - q$ is the zero vector.) This fact, plus the fact that o is equidistant from all the vertices of τ, implies that q is equidistant from all the vertices of τ (as Figure 4.5 demonstrates). Let r be the distance between q and any vertex of τ. As $q \in \tau$, there is no containment ball of τ (or σ) with radius less than r because q cannot move in any direction without moving away from some vertex of τ. Therefore, q and r are the center and radius of the min-containment ball of τ.

By the following reasoning, σ has the same min-containment ball as τ. If $q = o$, this conclusion is immediate. Otherwise, let h be the hyperplane through q orthogonal to oq. Observe that

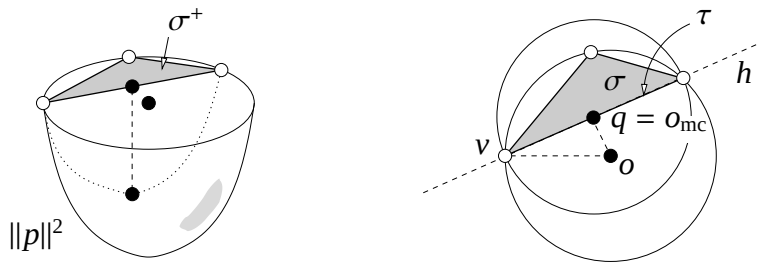

Figure 4.5: Left: within σ, the error $e(p)$ is maximized at the point nearest the circumcenter of σ. Right: top view of σ, its circumdisk, and its min-containment disk.

$\tau \subset h$. No point in σ is on the same side of h as o: if there were such a point w, there would be a point in σ (between w and q) closer to o than q, contradicting the fact that q is closest. The hyperplane h cuts the closed circumball of σ into two pieces, and the piece that includes σ is included in the min-containment ball of τ. Therefore, q and r are the center and radius of the min-containment ball of σ.

Let v be any vertex of τ. Pythagoras' Theorem on the triangle oqv (see Figure 4.5) yields $r_{\text{mc}}^2 = r^2 - d(o,q)^2$. □

Proposition 4.7. *Every Delaunay triangulation of S minimizes the largest min-containment ball, compared with all other triangulations of S.*

P . Over any single d-simplex σ, there is an explicit expression for $e(p)$. Recall from the proof of the Lifting Lemma (Lemma 2.1) that the hyperplane h_σ that includes σ^+ is defined by the function $h_\sigma(p) = 2\langle o, p\rangle - \|o\|^2 + r^2$, where o and r are the circumcenter and circumradius of σ and $p \in \mathbb{R}^d$ varies freely. Hence, for all $p \in \sigma$,

$$\begin{aligned} e(p) &= \mathcal{T}^+(p) - \|p\|^2 \\ &= h_\sigma(p) - \|p\|^2 \\ &= 2\langle o, p\rangle - \|o\|^2 + r^2 - \|p\|^2 \\ &= r^2 - d(o,p)^2. \end{aligned}$$

Figure 4.5 (left) illustrates the functions $h_\sigma(p)$ and $\|p\|^2$ over a triangle σ. The error $e(p)$ is the vertical distance between the two functions. At which point p in σ is $e(p)$ largest? At the point nearest the circumcenter o, because $d(o,p)^2$ is smallest there. (The error is maximized at $p = o$ if o is in σ; Figure 4.5 gives an example where it is not.) Let o_{mc} and r_{mc} be the center and radius of the min-containment ball of σ, respectively. By Proposition 4.6, the point in σ nearest o is o_{mc}, and $e(o_{\text{mc}}) = r^2 - d(o,o_{\text{mc}})^2 = r_{\text{mc}}^2$.

It follows that the square of the min-containment radius of σ is $r_{\text{mc}}^2 = \max_{p\in\sigma} e(p)$, and thus $\max_{p\in\text{conv}\,S} e(p)$ is the squared radius of the largest min-containment ball of the entire triangulation $\mathcal{T}$. By Proposition 4.5, the Delaunay triangulation minimizes this quantity among all triangulations of S. □

The optimality of the Delaunay triangulation for controlling the largest min-containment radius dovetails nicely with an error bound for piecewise linear interpolation derived by Waldron. Let $\mathcal{F}(c)$ be the space of scalar functions defined over $\operatorname{conv} S$ that are C^1-continuous and whose absolute curvature nowhere exceeds c. In other words, for every $f \in \mathcal{F}(c)$, every point $p \in \operatorname{conv} S$, and every unit direction vector $\vec{u}$, the magnitude of the second directional derivative $f''_{\vec{u}}(p)$ is at most c. This is a common starting point for analyses of piecewise linear interpolation error.

Let f be a function in $\mathcal{F}(c)$. Let $\sigma \subseteq \operatorname{conv} S$ be a simplex (of any dimensionality) with min-containment radius r_{mc}. Let h_σ be a linear function that interpolates f at the vertices of σ. Waldron shows that for all $p \in \sigma$, the absolute error $|e(p)| = |h_\sigma(p) - f(p)|$ is at most $cr_{\text{mc}}^2/2$. Furthermore, this bound is sharp: for every simplex σ with min-containment radius r_{mc}, there is a function $f \in \mathcal{F}(c)$ and a point $p \in \sigma$ such that $|e(p)| = cr_{\text{mc}}^2/2$. That function is $f(p) = c\|p\|^2/2$, as illustrated in Figure 4.5, and that point is $p = o_{\text{mc}}$.

Proposition 4.8. *Every Delaunay triangulation $\mathcal{T}$ of S minimizes* $\max_{f\in\mathcal{F}(c)} \max_{p\in\operatorname{conv} S} |\mathcal{T}^+(p) - f(p)|$*, the worst-case pointwise interpolation error, among all triangulations of S.*

P . Per Waldron, for any triangulation $\mathcal{T}$, $\max_{f\in\mathcal{F}(c)} \max_{p\in\operatorname{conv} S} |\mathcal{T}^+(p) - f(p)| = cr_{\text{max}}^2/2$, where r_{max} is the largest min-containment radius among all the simplices in $\mathcal{T}$. The result follows immediately from Proposition 4.7. □

One of the reasons for the longstanding popularity of Delaunay triangulations is that, as Propositions 4.5 and 4.8 show, the Delaunay triangulation is an optimal piecewise linear interpolating surface. Of course, $e(p)$ is not the only criterion for the merit of a triangulation used for interpolation. Many applications require that the interpolant approximate the gradient, i.e., $\nabla\mathcal{T}^+(p)$ must approximate $\nabla f(p)$ well. For the goal of approximating $\nabla f(p)$ in three or more dimensions, the Delaunay triangulation is sometimes far from optimal even for simple functions like the paraboloid $f(p) = \|p\|^2$. This is why eliminating slivers is a crucial problem in Delaunay mesh generation.

4.4 Bistellar flips and the flip algorithm

The flip algorithm described in Section 2.5 extends to three or more dimensions, but unfortunately, it does not always produce a Delaunay triangulation. The natural generalizations of edge flips are *bistellar flips*, operations that replace one set of simplices with another set filling the same volume. Figure 4.6 illustrates the bistellar flips in one, two, and three dimensions. The three-dimensional analogs of edge flips are called *2-3 flips* and *3-2 flips*. The names specify the numbers of tetrahedra deleted and created, respectively.

The upper half of the figure depicts basic bistellar flips, which retriangulate the convex hull of $d+2$ vertices in $\mathbb{R}^d$ by replacing a collection of k d-simplices with $d+2-k$ different d-simplices. In three dimensions, there are four basic flips: 1-4, 2-3, 3-2, and 4-1. The 1-4 flip inserts a vertex, and the 4-1 flip deletes one.

The lower half of the figure depicts extended bistellar flips, in which a lower-dimensional basic flip transforms higher-dimensional simplices, possibly many of them. For example, consider bisecting an edge of a tetrahedralization, as illustrated at the lower right of the figure. In essence, this operation is a one-dimensional 1-2 flip, replacing one edge with two. But every tetrahedron

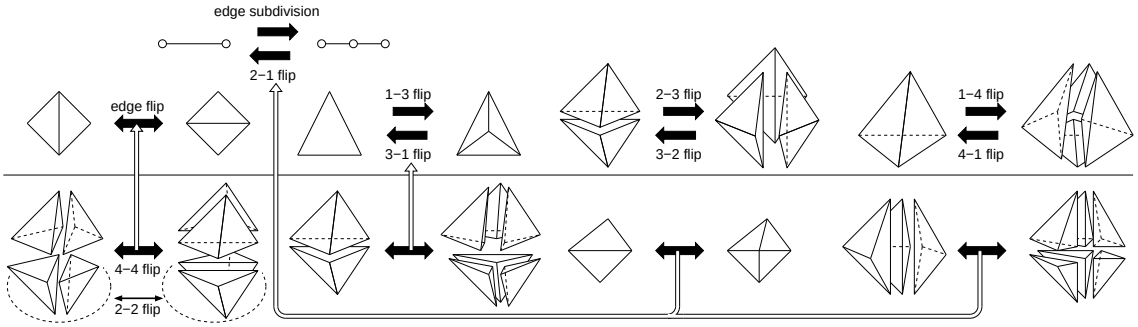

Figure 4.6: Basic bistellar flips in one, two, and three dimensions appear above the line. Extended bistellar flips appear below the line. White arrows connect extended flips to the lower-dimensional flips they are based on. The 2-2 flip at bottom left typically involves two coplanar triangular faces on the boundary of a domain, whereas the 4-4 flip occurs when the corresponding faces are in a domain interior. Edge subdivisions and their inverses can also occur on a domain boundary, as at bottom right, or in a domain interior.

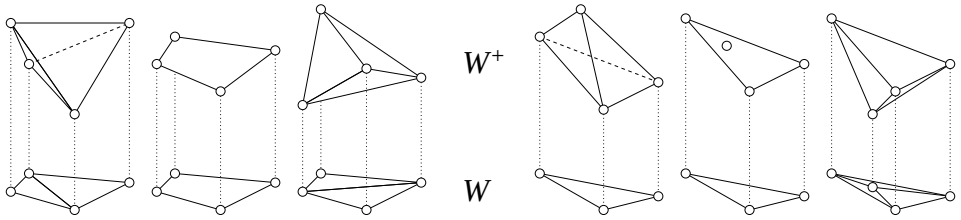

Figure 4.7: If the convex hull of four points in $\mathbb{R}^3$ is a tetrahedron, the facets on its underside determine one planar triangulation, and the facets on its upper side determine another.

that includes the subdivided edge is subdivided into two tetrahedra, and the number of tetrahedra that share the edge can be arbitrarily large. Therefore, some extended flips can delete and create arbitrarily many d-simplices.

An intuitive way to understand the basic bistellar flips in $\mathbb{R}^d$ is through the faces of a simplex in $\mathbb{R}^{d+1}$, as illustrated in Figure 4.7. Let W be a set of $d+2$ points in $\mathbb{R}^d$, and let W^+ be the same points lifted by the parabolic lifting map in $\mathbb{R}^{d+1}$. Call the $(d+1)$th coordinate axis (along which the points are lifted) the *vertical axis*. Assume the points in W are not cospherical. Then the points in W^+ are not cohyperplanar, and $\operatorname{conv} W^+$ is a $(d+1)$-simplex—call it the *W-simplex*. Each facet of the W-simplex can be placed in one of three classes: vertical (parallel to the vertical axis), lower (facing the negative end of the vertical axis), or upper (those that would get wet if rain were falling).

The W-simplex suggests two different triangulations of the region $\operatorname{conv} W$: the Delaunay triangulation by projecting the lower facets of $\operatorname{conv} W^+$ to $\mathbb{R}^d$, and a non-Delaunay triangulation by projecting the upper facets. (If the points in W^+ are cohyperplanar, W has two Delaunay triangulations.) The act of replacing one such triangulation with the other is a bistellar flip. If the W-simplex has no vertical facet, the flip is basic. These are the only two ways to triangulate $\operatorname{conv} W$ such that all the vertices are in W. One of the two triangulations might omit a vertex of

W—witness the 3-1 flip, which deletes a vertex.

An extended bistellar flip in $\mathbb{R}^d$ is built on a j-dimensional basic flip as follows. Consider a basic flip that replaces a set T_D of k j-simplices with a set T_C of $j+2-k$ j-simplices. Let the *join* $\tau * \zeta$ of two disjoint simplices τ and ζ be the simplex $\operatorname{conv}(\tau \cup \zeta)$ having all the vertices of τ and ζ, and let the *join* of two sets T and Z of simplices be the set of simplices $\{\tau * \zeta : \tau \in T \text{ and } \zeta \in Z\}$. Let Z be a set of $(d-j-1)$-simplices such that every member of $T_D * Z$ is a nondegenerate d-simplex and $T_D * Z$ contains every d-simplex in $\mathcal{T}$ with a face in T_D. If such a Z exists, the act of replacing the simplices $T_D * Z$ with the simplices $T_C * Z$ is an extended flip. For example, in the edge bisection illustrated at the lower right of Figure 4.6, T_D contains just the bisected edge, T_C contains the two edges the bisection yields, and Z contains one edge for each bisected tetrahedron.

The flip algorithm requires a solution to the following problem. A triangulation $\mathcal{T}$ has a facet f that is not locally Delaunay. What is the appropriate flip to eliminate f? Let W be the set containing the d vertices of f and the two additional vertices of the two d-simplices having f for a face. The fact that f is not locally Delaunay implies that f^+ lies on the upper surface of the W-simplex $\operatorname{conv} W^+$. The upper facets of the W-simplex indicate which d-simplices the flip algorithm should delete from $\mathcal{T}$ (including the two adjoining f), and the lower facets indicate which d-simplices should replace them. The procedure F in Figure 4.8 identifies these tetrahedra for $d = 3$. If the W-simplex has vertical facets, F performs an extended flip.

The difficulty is that the simplices to be deleted might not all be in $\mathcal{T}$. Figure 4.9 illustrates circumstances where the flip algorithm wishes to perform a flip, but cannot. At left, the shaded triangle is not locally Delaunay. The right flip to remove it is a 3-2 flip, but the flip is possible only if the third tetrahedron is present. If four or more tetrahedra share the bold edge, the flip is blocked, at least until another flip creates the missing tetrahedron. The flip algorithm can get stuck in a configuration where *every* locally non-Delaunay triangle's removal is blocked, and the algorithm cannot make further progress toward the Delaunay triangulation. This is not a rare occurrence in practice.

If the flip algorithm is asked to compute a *weighted* Delaunay triangulation, it must sometimes perform a flip that deletes a vertex, such as the 4-1 flip illustrated at right in Figure 4.9. Such a flip is possible only if all the simplices the flip is meant to delete are present. Even in the plane, there are circumstances where every desired 3-1 flip is blocked and the flip algorithm is stuck.

Extended flips are even more delicate; they require not only that $T_D * Z \subseteq \mathcal{T}$, but also that $T_D * Z$ contains *every* tetrahedron in $\mathcal{T}$ that has a face in T_D.

Whether it succeeds or gets stuck, the running time of the flip algorithm is $O(n^{1+\lfloor d/2 \rfloor})$, by the same reasoning explained in Section 2.5: a flip can be modeled as the act of gluing a $(d+1)$-simplex to the underside of the lifted triangulation, and a triangulation in $\mathbb{R}^{d+1}$ has at most $O(n^{1+\lfloor d/2 \rfloor})$ simplices.

One of the most important open problems in combinatorial geometry asks whether the *flip graph* is connected. For a specified point set, the flip graph has one node for every triangulation of those points. Two nodes are connected by an edge if one triangulation can be transformed into the other by a single bistellar flip, excluding those flips that create or delete a vertex. For every planar point set, its flip graph is connected—in other words, any triangulation of the points can be transformed into any other triangulation of the same points by a sequence of edge flips. One way to see this is to recall that Proposition 2.5 states that every triangulation can be flipped to the Delaunay triangulation. However, there exist point sets in five or more dimensions whose flip

```
F   (𝒯, uvw)
1.      x ← A          (u, v, w)
2.      y ← A          (w, v, u)
3.      T_D ← {wvuy, uvwx}      { delete tetrahedra wvuy and uvwx }
4.      T_C ← ∅
5.      V ← ∅
6.      For (a, b, c) ← (u, v, w), (v, w, u), and (w, u, v)
7.          α ← O      3D(a, b, x, y)
8.          If α > 0
9.              T_D ← T_D ∪ {abxy}      { delete tetrahedron abxy }
10.         else if α < 0
11.             T_C ← T_C ∪ {abyx}      { create tetrahedron abyx }
12.         else V ← V ∪ {c}      { abxy is degenerate and c is not part of the basic flip }
        { perform a flip that replaces T_D with T_C }
13.     If V = ∅      { basic flip: 2-3 flip or 3-2 flip or 4-1 flip }
            { note: if any simplex in T_D is absent from 𝒯, the flip is blocked }
14.         For each τ ∈ T_D
15.             Call D      T          (τ)
16.         For each τ ∈ T_C
17.             Call A   T          (τ)
18.     else      { extended flip: 2-2 flip or 4-4 flip or 3-1 flip or 6-2 flip or edge merge }
19.         j ← 3 − |V|
20.         Remove the vertices in V from every simplex in T_D and T_C, yielding j-simplices
21.         σ ← a j-simplex in T_D
22.         For each (d − j − 1)-simplex ζ such that σ ∗ ζ is a tetrahedron in 𝒯
23.             For each τ ∈ T_D
                    { note: if τ ∗ ζ is absent from 𝒯, the flip is blocked }
24.                 Call D      T          (τ ∗ ζ)
25.             For each τ ∈ T_C
26.                 Call A   T          (τ ∗ ζ)
```

Figure 4.8: Algorithm for performing a tetrahedral bistellar flip. The parameters to F are a triangulation $\mathcal{T}$ and a facet $uvw \in \mathcal{T}$ to flip. F assumes uvw can be flipped; comments identify places where this assumption could fail.

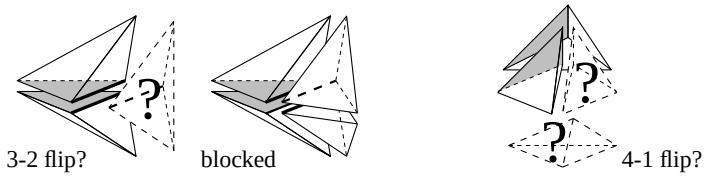

Figure 4.9: The shaded facet at left is not locally Delaunay. It can be removed by a 3-2 flip, but only if the third tetrahedron is present; the flip is blocked if more than three tetrahedra share the central edge (bold). The shaded facet at right can be removed by a 4-1 flip if the other two tetrahedra are present.

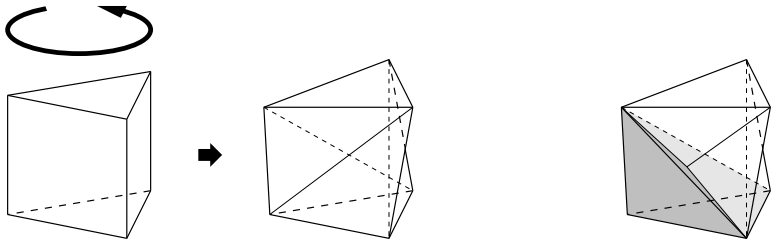

Figure 4.10: Schönhardt's untetrahedralizable polyhedron (center) is formed by rotating one end of a triangular prism (left), thereby creating three diagonal reflex edges. The convex hull of any four polyhedron vertices (right) sticks out.

graphs are not connected; they have triangulations that cannot be transformed to Delaunay by a sequence of bistellar flips. The question remains open in three and four dimensions. But even if all flip graphs for three-dimensional point sets are connected, flipping facets that are locally non-Delaunay does not suffice to find the Delaunay triangulation.

Despite the failure of the flip algorithm for three-dimensional Delaunay triangulations and weighted two-dimensional Delaunay triangulations, some Delaunay triangulation algorithms rely on bistellar flips, including several incremental vertex insertion algorithms and an algorithm for inserting a polygon into a CDT, the latter described in Section 5.8. In particular, if a new vertex is introduced into a Delaunay triangulation by a simple 1-4 flip (or by subdividing a facet or edge of the triangulation), and the flip algorithm is run before the triangulation is changed in any other way, the flip algorithm is guaranteed to restore the Delaunay property without getting stuck.

4.5 Three-dimensional constrained Delaunay triangulations

Constrained Delaunay triangulations generalize to three or more dimensions, but whereas every piecewise linear complex in the plane has a CDT, not every three-dimensional PLC has one. Worse yet, there exist simple polyhedra that do not have triangulations at all—that is, they cannot be subdivided into tetrahedra without creating new vertices (i.e. tetrahedron vertices that are not vertices of the polyhedron).

E. Schönhardt furnishes an example depicted in Figure 4.10. The easiest way to envision this polyhedron is to begin with a triangular prism. Imagine grasping the prism so that its bottom triangular face cannot move, while twisting the top triangular face so it rotates slightly about its center while remaining horizontal. This rotation breaks each of the three square faces into two triangular faces along a diagonal *reflex edge*—an edge at which the polyhedron is locally nonconvex. After this transformation, the upper left corner and lower right corner of each (former) square face are separated by a reflex edge and are no longer visible to each other within the polyhedron. Any four vertices of the polyhedron include two separated by a reflex edge; thus, any tetrahedron whose vertices are vertices of the polyhedron does not lie entirely within the polyhedron. Therefore, Schönhardt's polyhedron cannot be triangulated without additional vertices. It can be subdivided into tetrahedra with the addition of one vertex at its center.

Adding to the difficulty, it is NP-hard to determine whether a polyhedron has a triangulation, or whether it can be subdivided into tetrahedra with only k additional vertices for an arbitrary

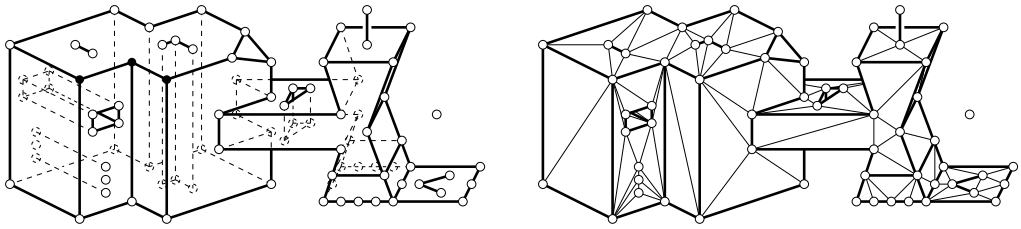

Figure 4.11: A three-dimensional piecewise linear complex and its constrained Delaunay triangulation. Each polygon and polyhedron may have holes, slits, and vertices in its relative interior. Each polyhedron may also have polygons in its interior.

constant k.

The following sections discuss triangulations and CDTs of polyhedra and PLCs in three dimensions. It is possible to refine any polyhedron or PLC by adding new vertices on its edges so that it has a constrained Delaunay triangulation. This fact makes CDTs useful in three dimensions.

4.5.1 Piecewise linear complexes and their triangulations in $\mathbb{R}^d$

The domain over which a general-dimensional CDT is defined is a general-dimensional piecewise linear complex, which is a set of linear cells—vertices, edges, polygons, and polyhedra—as illustrated in Figure 4.11. The linear cells constrain how the complex can be triangulated: each linear cell in the complex must be a union of simplices in the triangulation. The union of the linear cells specifies the region to be triangulated.

Definition 4.3 (piecewise linear complex)**.** A *piecewise linear complex* (PLC) $\mathcal{P}$ is a finite set of linear cells that satisfies the following properties.

- The vertices and edges in $\mathcal{P}$ form a simplicial complex.
- For each linear cell $f \in \mathcal{P}$, the boundary of f is a union of linear cells in $\mathcal{P}$.
- If two distinct linear cells $f, g \in \mathcal{P}$ intersect, their intersection is a union of linear cells in $\mathcal{P}$, all having lower dimension than at least one of f or g.

As in the plane, the edges in $\mathcal{P}$ are called *segments*. Its *underlying space* is $|\mathcal{P}| = \bigcup_{f\in\mathcal{P}} f$, which is usually the domain to be triangulated. The *faces* of a linear cell $f \in \mathcal{P}$ are the linear cells in $\mathcal{P}$ that are subsets of f, including f itself.

A triangulation of a PLC must cover every polyhedron, respect every polygon, and include every segment and vertex.

Definition 4.4 (triangulation of a PLC)**.** Let $\mathcal{P}$ be a PLC. A *triangulation of* $\mathcal{P}$ is a simplicial complex $\mathcal{T}$ such that $\mathcal{P}$ and $\mathcal{T}$ have the same vertices, every linear cell in $\mathcal{P}$ is a union of simplices in $\mathcal{T}$, and $|\mathcal{T}| = |\mathcal{P}|$.

Because this definition does not allow $\mathcal{T}$ to have new vertices absent from $\mathcal{P}$, every edge in $\mathcal{P}$ must appear in $\mathcal{T}$. However, the polygons in $\mathcal{P}$ may be subdivided into triangles in $\mathcal{T}$.

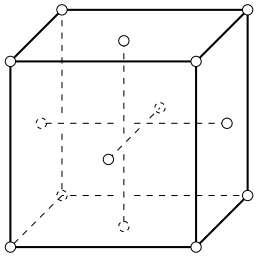

Figure 4.12: A convex PLC with no triangulation.

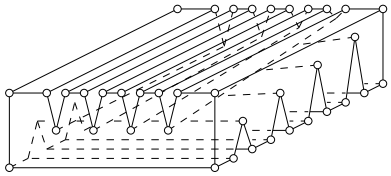

Figure 4.13: Chazelle's polyhedron.

Schönhardt's polyhedron shows that not every PLC has a triangulation. Every convex polyhedron has a triangulation; what about convex polyhedra with internal segments? Figure 4.12 illustrates a PLC with no triangulation, consisting of a cube inside which three orthogonal segments pass by each other but do not intersect. If any one of the segments is omitted, the PLC has a triangulation. This example shows that, unlike with planar triangulations, it is not always possible to insert a new edge into a tetrahedralization.

Because some polyhedra and PLCs do not have triangulations, Steiner triangulations are even more important in three dimensions than in the plane.

Definition 4.5 (Steiner triangulation of a PLC)**.** Let $\mathcal{P}$ be a PLC. A *Steiner triangulation of* $\mathcal{P}$, also known as a *conforming triangulation of* $\mathcal{P}$ or a *mesh of* $\mathcal{P}$, is a simplicial complex $\mathcal{T}$ such that $\mathcal{T}$ contains every vertex in $\mathcal{P}$ and possibly more, every linear cell in $\mathcal{P}$ is a union of simplices in $\mathcal{T}$, and $|\mathcal{T}| = |\mathcal{P}|$. The new vertices in $\mathcal{T}$, not present in $\mathcal{P}$, are called *Steiner points*. A *Steiner Delaunay triangulation* of $\mathcal{P}$, also known as a *conforming Delaunay triangulation* of $\mathcal{P}$, is a Steiner triangulation of $\mathcal{P}$ in which every simplex is Delaunay.

Every n-vertex polyhedron has a Steiner triangulation with at most $O(n^2)$ vertices, found by constructing a *vertical decomposition* of the polyhedron. The same is true for PLCs of complexity n. Unfortunately, there are polyhedra for which it is not possible to do better; Figure 4.13 depicts Chazelle's polyhedron, which has n vertices and $O(n)$ edges, but cannot be divided into fewer than $\Theta(n^2)$ convex bodies. The worst-case complexity of subdividing a polyhedron is related to its number of reflex edges: there is an algorithm that divides any polyhedron with r reflex edges into $O(n + r^2)$ tetrahedra, and some polyhedra with r reflex edges cannot be divided into fewer than $\Omega(n + r^2)$ convex bodies.

It appears likely, though it is proved only in two dimensions, that there exist PLCs whose smallest Steiner Delaunay triangulations are asymptotically larger than their smallest Steiner triangulations. There are algorithms that can find a Steiner Delaunay tetrahedralization of any three-dimensional polyhedron, but they might introduce a superpolynomial number of new vertices. No

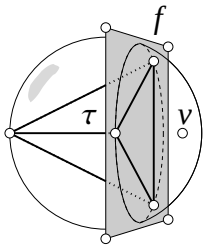

Figure 4.14: A constrained Delaunay tetrahedron τ.

known algorithm for finding Steiner Delaunay tetrahedralizations is guaranteed to introduce only a polynomial number of new vertices, and no algorithm of any complexity has been offered for four- or higher-dimensional Steiner Delaunay triangulations. Moreover, the existing algorithms all seem to introduce an unnecessarily large number of vertices near small domain angles. These problems can be partly remediated by Steiner CDTs.

4.5.2 The constrained Delaunay triangulation in $\mathbb{R}^3$

Three-dimensional constrained Delaunay triangulations aspire to retain most of the advantages of Delaunay triangulations while respecting constraints. But Figures 4.10, 4.12, and 4.13 demonstrate that some PLCs, even some polyhedra, have no triangulation at all. Moreover, some polyhedra that do have triangulations do not have CDTs. Nevertheless, CDTs are useful because, if we are willing to add new vertices, every three-dimensional PLC has a Steiner CDT, and a Steiner CDT might require many fewer vertices than a Steiner Delaunay triangulation.

As in the plane, there are several equivalent definitions of "constrained Delaunay triangulation" in three dimensions. The simplest is that a CDT is a triangulation of a PLC in which every facet not included in a PLC polygon is locally Delaunay. A CDT differs from a Delaunay triangulation in three ways: it is not necessarily convex, it is required to respect a PLC, and the facets of the CDT that are included in PLC polygons are exempt from being locally Delaunay.

Recall from Definition 2.11 that a simplex σ *respects* a PLC $\mathcal{P}$ if $\sigma \subseteq |\mathcal{P}|$ and for every $f \in \mathcal{P}$ that intersects σ, $f \cap \sigma$ is a union of faces of σ. By Definition 2.13, two points x and y are *visible* to each other if xy respects $\mathcal{P}$. A linear cell in $\mathcal{P}$ that intersects the relative interior of xy but does not include xy *occludes* the visibility between x and y. The primary definition of CDT specifies that every tetrahedron is constrained Delaunay, defined as follows.

Definition 4.6 (constrained Delaunay)**.** In the context of a PLC $\mathcal{P}$, a simplex σ is *constrained Delaunay* if $\mathcal{P}$ contains the vertices of σ, σ respects $\mathcal{P}$, and there is an open circumball of σ that contains no vertex in $\mathcal{P}$ that is visible from any point in the relative interior of σ.

Figure 4.14 depicts a constrained Delaunay tetrahedron τ. Every face of τ whose relative interior intersects the polygon f is included in f, so τ respects $\mathcal{P}$. The open circumball of τ contains one vertex v, but v is not visible from any point in the interior of τ, because f occludes its visibility.

Definition 4.7 (constrained Delaunay triangulation)**.** Let $\mathcal{P}$ be a three-dimensional PLC. A *constrained Delaunay triangulation* (CDT) of $\mathcal{P}$ is a triangulation of $\mathcal{P}$ in which every tetrahedron

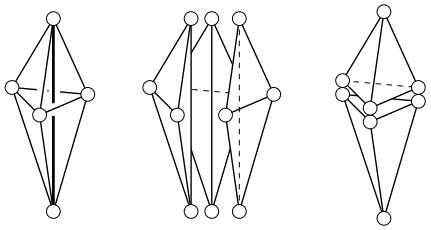

Figure 4.15: Left: a PLC with no CDT. Center: the sole tetrahedralization of this PLC. Its three tetrahedra are not constrained Delaunay. Right: the two Delaunay tetrahedra do not respect the central segment.

is constrained Delaunay, and every dangling triangle (i.e. not a face of any tetrahedron) is also constrained Delaunay.

Figure 4.11 illustrates a PLC and its CDT. Observe that the PLC has a polygon that is not a face of any polyhedron; this face is triangulated with constrained Delaunay triangles.

Figure 4.15 illustrates a PLC that has no CDT because of a segment that runs vertically through the domain interior. There is only one tetrahedralization of this PLC—composed of three tetrahedra encircling the central segment—and its tetrahedra are not constrained Delaunay, because each of them has a visible vertex in its open circumball. Whereas polygons usually block enough visibility to ensure their presence in a CDT, segments usually do not. But segments can dictate that a CDT does not exist at all. If the central segment in Figure 4.15 is removed, the PLC has a CDT made up of two tetrahedra.

A *Steiner CDT* or *conforming CDT* of $\mathcal{P}$ is a Steiner triangulation of $\mathcal{P}$ in which every tetrahedron is constrained Delaunay, and every dangling triangle (i.e. not a face of any tetrahedron) is also constrained Delaunay. A PLC with no CDT has a Steiner CDT, but one or more Steiner points must be added on its segments. For example, the PLC in Figure 4.15 has a Steiner CDT with one Steiner point on its central segment.

4.5.3 The CDT Theorem

Although not all piecewise linear complexes have constrained Delaunay triangulations, there is an easy-to-test, sufficient (but not necessary) condition that guarantees that a CDT exists. A three-dimensional PLC $\mathcal{P}$ is *edge-protected* if every edge in $\mathcal{P}$ is strongly Delaunay.

Theorem 4.9 (CDT Theorem)**.** *Every edge-protected PLC has a CDT.* □

It is not sufficient for every edge in $\mathcal{P}$ to be Delaunay. If all six vertices of Schönhardt's polyhedron lie on a common sphere, then all of its edges (and all its faces) are Delaunay, but it still has no tetrahedralization. It is not possible to place the vertices of Schönhardt's polyhedron so that all three of its reflex edges are strongly Delaunay, though any two may be.

What if a PLC that one wishes to triangulate is not edge-protected? One can make it edge-protected by adding vertices on its segments—a task that any Delaunay mesh generation algorithm must do anyway. The augmented PLC has a CDT, which is a Steiner CDT of the original PLC.

Figure 4.16 illustrates the difference between using a Delaunay triangulation and using a CDT for mesh generation. With a Delaunay triangulation, the mesh generator must insert new vertices

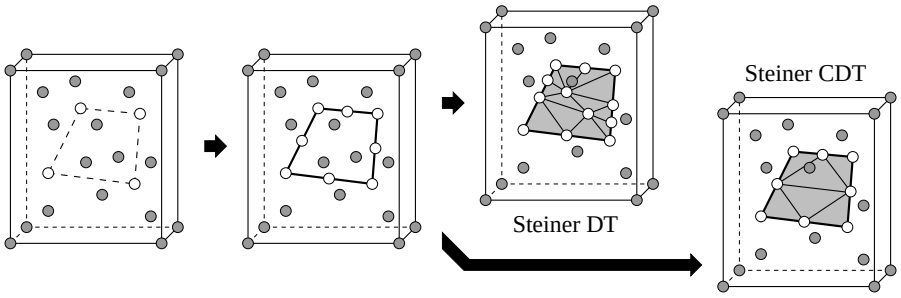

Figure 4.16: Comparison of Steiner Delaunay triangulations and Steiner CDTs. For clarity, vertices inside each box are shown, but tetrahedra are not. For both types of triangulation, missing segments are recovered by inserting new vertices until each segment is a union of strongly Delaunay edges. In a Steiner Delaunay triangulation, additional vertices are inserted until each polygon is a union of strongly Delaunay triangles. In a Steiner CDT, no additional vertices need be inserted; the polygons are recovered by computing a CDT.

that guarantee that every segment is a union of Delaunay (preferably strongly Delaunay) edges, and every polygon is a union of Delaunay (preferably strongly Delaunay) triangles. With a CDT, new vertices must be inserted that guarantee that every segment is a union of strongly Delaunay edges; but then the augmented PLC is edge-protected, and the CDT Theorem guarantees that the polygons can be recovered without inserting any additional vertices. The advantage of a CDT is that many fewer vertices might be required.

Testing whether a PLC $\mathcal{P}$ is edge-protected is straightforward. Form the Delaunay triangulation of the vertices in $\mathcal{P}$. If a segment $\sigma \in \mathcal{P}$ is missing from the triangulation, then σ is not strongly Delaunay, and $\mathcal{P}$ is not edge-protected. If σ is present, it is Delaunay. If the symbolic perturbations described in Section 2.9 are used to make the vertices in $\mathcal{P}$ generic, then every Delaunay edge is strongly Delaunay; so if every segment in $\mathcal{P}$ is present, $\mathcal{P}$ is edge-protected. (If symbolic perturbations are not used, then testing whether a Delaunay segment σ is strongly Delaunay is equivalent to determining whether the Voronoi polygon dual to σ is nondegenerate.)

4.5.4 Properties of the constrained Delaunay triangulation in $\mathbb{R}^3$

This section summarizes the properties of three-dimensional CDTs.

The Delaunay Lemma for three-dimensional CDTs provides an alternative definition of CDT: a triangulation of a PLC $\mathcal{P}$ is a CDT if and only if every one of its facets is locally Delaunay *or* is included in a polygon in $\mathcal{P}$.

Lemma 4.10 (Constrained Delaunay Lemma)**.** *Let $\mathcal{P}$ be a PLC in which every linear cell is a face of some polyhedron in $\mathcal{P}$, so there are no dangling polygons. Let $\mathcal{T}$ be a triangulation of $\mathcal{P}$. The following three statements are equivalent.*

(i) *Every tetrahedron in $\mathcal{T}$ is constrained Delaunay (i.e. $\mathcal{T}$ is constrained Delaunay).*

(ii) *Every facet in $\mathcal{T}$ not included in a polygon in $\mathcal{P}$ is constrained Delaunay.*

(iii) *Every facet in $\mathcal{T}$ not included in a polygon in $\mathcal{P}$ is locally Delaunay.* □

A constrained Delaunay triangulation $\mathcal{T}$ of $\mathcal{P}$ induces a two-dimensional triangulation of each polygon $f \in \mathcal{P}$, namely $\mathcal{T}|_f = \{\sigma \in \mathcal{T} : \sigma \subseteq f\}$. Statement (ii) above implies that the triangles in $\mathcal{T}|_f$ need not be constrained Delaunay with respect to $\mathcal{P}$—but they *are* constrained Delaunay with respect to the polygon f, in the following sense.

Proposition 4.11. *Let $\mathcal{T}$ be a CDT of a three-dimensional PLC $\mathcal{P}$. Let $f \in \mathcal{P}$ be a polygon. Let $\mathcal{T}|_f$ be the set of simplices in $\mathcal{T}$ that are included in f. Let $\mathcal{P}|_f$ be the set of faces of f (including f itself); $\mathcal{P}|_f$ is a two-dimensional PLC embedded in three-dimensional space. Then $\mathcal{T}|_f$ is a CDT of $\mathcal{P}|_f$.* □

A PLC is *generic* if its vertices are generic. A generic PLC has a unique CDT, if it has one at all.

Proposition 4.12. *A generic piecewise linear complex has at most one constrained Delaunay triangulation.* □

A consequence of Propositions 4.11 and 4.12 is that, if a PLC is generic, a CDT construction algorithm can begin by computing the two-dimensional CDTs of the polygons, then use them to help compute the three-dimensional CDT of the PLC, secure in the knowledge that the polygon triangulations will match the volume triangulation.

CDTs inherit the optimality properties of Delaunay triangulations described in Section 4.3, albeit with respect to a smaller set of triangulations, namely the triangulations of a PLC. However, if a PLC has no CDT, finding the optimal triangulation is an open problem.

Proposition 4.13. *Let $\mathcal{P}$ be a PLC. If $\mathcal{P}$ has a CDT, then every CDT of $\mathcal{P}$ minimizes the largest min-containment ball, compared with all other triangulations of $\mathcal{P}$. Every CDT of $\mathcal{P}$ also optimizes the criteria discussed in Propositions 4.5 and 4.8.* □

4.6 Notes and exercises

The upper bound of $\Theta(n^{\lceil d/2 \rceil})$ simplices in an n-vertex triangulation follows from McMullen's celebrated Upper Bound Theorem [145] of 1970. Seidel [191] gives a one-paragraph proof of the asymptotic bound.

Rajan [173] shows that the Delaunay triangulation minimizes the largest min-containment ball in any dimensionality, thereby generalizing the two-dimensional result of D'Azevedo and Simpson [67] and yielding Proposition 4.7. For an algebraic proof of Proposition 4.6 based on quadratic program duality, see Lemma 3 of Rajan [173]. Rippa [176] shows that the Delaunay triangulation in the plane minimizes the piecewise linear interpolation error for bivariate functions of the form $Ax^2 + Ay^2 + Bx + Cy + D$, measured in the L_q-norm for every $q \geq 1$, and Melissaratos [146] generalizes Rippa's result to higher dimensions, yielding Proposition 4.5. Shewchuk [204] extends all these optimality results to CDTs. The error bound for piecewise linear interpolation given in Section 4.3 is by Waldron [221].

Lawson [132] proves the claim from Section 4.4 that there are only two triangulations of the configuration of vertices involved in a basic bistellar flip. An earlier paper by Lawson [130] shows that for every planar point set, the flip graph is connected. Santos [184, 185] gives examples of point sets in five or more dimensions whose flip graphs are not connected. Joe [118] gives an

example of a tetrahedralization for which the flip algorithm is stuck and can make no progress toward the Delaunay tetrahedralization. Edelsbrunner and Shah [91] give an example of a triangulation in the plane and a set of weights for which the flip algorithm is stuck and can make no progress toward the weighted Delaunay triangulation. The fact that the flip algorithm does not get stuck after a single vertex is introduced into a Delaunay triangulation by subdivision is proved by Joe [119], and by Edelsbrunner and Shah [91] for weighted Delaunay triangulations.

Schönhardt's polyhedron was discovered by Schönhardt [187], and Chazelle's polyhedron by Chazelle [44]. The NP-hardness of determining whether a polyhedron has a triangulation, cited in Section 4.5, is proved by Ruppert and Seidel [181]. Chazelle [44] proposes the vertical decomposition of a polyhedron, and Chazelle and Palios [45] give an algorithm that subdivides any n-vertex polyhedron with r reflex edges into $O(n + r^2)$ tetrahedra. This bound is optimal for the worst polyhedra.

The notion of a PLC was proposed by Miller, Talmor, Teng, Walkington, and Wang [149].[1]

Algorithms for computing a Steiner Delaunay triangulation of a PLC include those by Murphy, Mount, and Gable [156], Cohen-Steiner, Colin de Verdière, and Yvinec [65], Cheng and Poon [56], Cheng, Dey, Ramos, and Ray [52], and Rand and Walkington [174]. None has a polynomial bound on the number of new vertices.

CDTs were generalized to three or more dimensions by Shewchuk [204], whose paper includes proofs of the CDT Theorem and the properties of three-dimensional CDTs given in Section 4.5.4.

Exercises

1. Definition 4.3 of *piecewise linear complex* implies that if the interior of a segment intersects the interior of a polygon, the segment is entirely included in the polygon. Prove it.

2. Show that the edges and triangular faces of a strongly Delaunay tetrahedron are strongly Delaunay.

3. Prove Proposition 4.2. Consult Figure 2.10 for inspiration.

4. Prove Proposition 4.11.

5. Exercise 7 in Chapter 2 asks for a proof of a fact about constrained Delaunay triangles in the plane. Give a counterexample that demonstrates that the analogous fact is *not* true of constrained Delaunay tetrahedra in three dimensions.

6. Design an algorithm that adds vertices to a three-dimensional PLC so that the augmented PLC has a CDT.

[1] Miller et al. call it a *piecewise linear system*, but their construction is so obviously a complex that a change in name seems obligatory. Our definition is different from that of Miller et al., but nearly equivalent, with one true difference: Miller et al. do not impose the restriction that the vertices and edges form a simplicial complex; they permit vertices to lie in the relative interior of an edge. Disallowing such vertices simplifies our presentation while entailing no essential loss of generality, because edges with vertices in their relative interiors can be subdivided into edges that obey the restriction.